OPTIMAL DESIGN OF HEXAPOD WALKING ROBOT LEG STRUCTURE BASED ON ENERGY CONSUMPTION AND WORKSPACE

Ya-guang Zhu, Bo Jin, Wei Li and Shi-tong Li
The State Key Lab of Fluid Power Transmission and Control, Zhejiang University, Hangzhou, China
E-mail: bjin@zju.edu.cn

Received April 2013, Accepted March 2014
No. 13-CSME-125, E.I.C. Accession 3583

ABSTRACT

In order to achieve the optimal design of the hexapod walking robot leg structure, a combined index of energy consumption and workspace is raised. By deriving the energy consumption functions and analyzing the target workspace, a mathematical model of nonlinear programming with inequality constraints is established. The genetic algorithm coupled with inverse kinematics and trajectory planning in a gait period is utilized to solve the optimization problem. The analysis verifies that the requirements of turning and obstacle overcoming can be satisfied, and the total energy consumption can be reduced. The results show that the optimal parameters not only satisfy the requirement of the target workspace, but also achieve the minimum energy consumption and lower joint torques.

Keywords: hexapod walking robot; optimal design; energy consumption; workspace.

CONCEPTION OPTIMALE DE LA STRUCTURE D'UNE JAMBE DE ROBOT MARCHEUR HEXAPODE BASÉE SUR LA CONSOMMATION D'ÉNERGIE ET L'ESPACE DE TRAVAIL

RÉSUMÉ

Dans le but de réaliser une conception optimale d'une jambe de robot marcheur hexapode, un index combiné de consommation d'énergie et d'espace de travail est invoqué. En dérivant les fonctions de consommation d'énergie et en analysant l'espace de travail visé, un modèle mathématique d'un programme non-linéaire avec contraintes de programmation inégales est établi. L'algorithme génétique couplé avec la cinématique inverse et la planification de trajectoire de la démarche est utilisé pour résoudre le problème d'optimisation. L'analyse vérifie que les exigences des mouvements de virage et les obstacles à éviter sont satisfaits, et que la consommation d'énergie totale peut tre réduite. Les résultats démontrent que les parameters optimaux ne font pas que satisfaire les exigences de l'espace de travail visé mais aussi une consommation d'énergie minimum et des moments de torsion de l'articulation moins élevés.

Mots-clés : robot marcheur hexapode; conception optimale; consommation d'énergie; espace de travail.

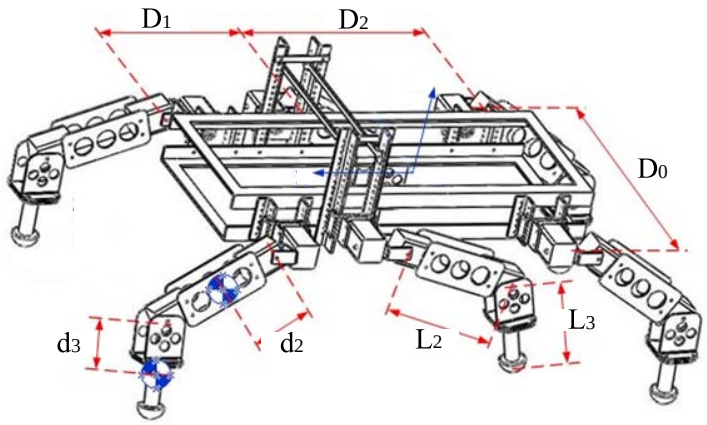

Fig. 1. Mechanical model of hexapod walking robot.

1. INTRODUCTION

In recent years, multi-legged walking robot is broadly recognized for superior performance as an effective and efficient transportation device on irregular or difficult terrains. The possible application areas for legged robots include the explorations of volcanoes [1], searching and rescue missions [2] humanitarian demining [3] or other exploration missions [4]. Most of these circumstances usually go along with hazardous and unstructured, complex environments, which cannot be entered by humans. Compared with wheeled or tracked locomotion, legged robots have variety of advantages on coping with these scenarios [5]. Various hexapod walking robots have been developed in the past 30 years [6–8].

For multi-legged walking robots, mechanism design is the base of the integral structure, gait generation and control of system. In this respect, Gosselin [9] firstly put forward the global performance index (GCI) which combines Jacobian matrix condition number and workspace. This method is widely used. Lan et al. [10] raised performance index including velocity and dexterity and Liu et al. [[11] considered some performance index including workspace, singularity, isotropy. Optimal design of parallel robot with time-invariant posture space, GCI and time-varying posture space is raised by Hwang et al. [12]. Oetomo et al. [13] proposed a kind of design method for series mechanisms based on region search. Many other methods also received good results in the design of multi-legged walking robots [14–16]. Our recently published paper [17] performed the energy efficiency analysis of hexapod walking robot and proposed the torque distribution algorithm to minimize the system's energetic cost. The research objective was the whole robot. However, this paper mainly focuses on the energy consumption and workspace of a single leg, and raises an optimal design approach of the leg. The ability of striding over obstacles and reducing the overall energy consumption is taken into consideration. The combined index based on system energy consumption and target workspace is raised and used in the optimization objective function. After optimizing the structural parameters using genetic algorithm, the minimum system energy consumption is achieved and the requirement of the target workspace is satisfied.

The paper is structured as follows: in Section 2, the overall structure is configured and the model of leg is built and analyzed. Section 3 shows the combined index of the energy consumption and the workspace, and the constraints are presented. In Section 4, the optimization is realized using G.A, and the result is analyzed. Section 5 is the summary of the whole work.

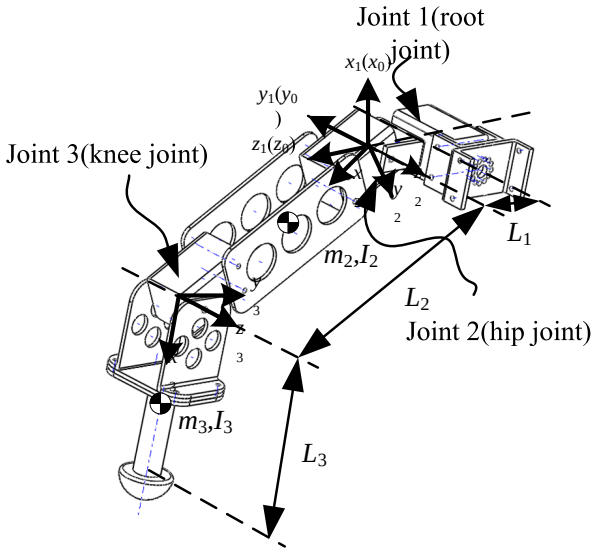

Fig. 2. Three-joint robot leg: Reference frames and joint variables.

Table 1. Denavit–Hartenberg link parameters for three joint robot legs.

Linkage j	$\alpha_{ij}/^\circ$	d_{ij}/m	a_{ij}/m	$\theta_{ij}/^\circ$
1	90°	0	0	$\theta_{i1\min} \sim \theta_{i1\max}$ $(i=1,2,3)/-\theta_{i1\max} \sim -\theta_{i1\min}$ $(i=4,5,6)$
2	0	0	L_2	$\theta_{i2\min} \sim \theta_{i2\max}$ $(i=2,3,4,5)/-\theta_{i2\max} \sim -\theta_{i2\min}$ $(i=1,6)$
3	0	0	L_3	$\theta_{i3\min} \sim \theta_{i3\max}$ $(i=2,3,4,5)/-\theta_{i3\max} \sim -\theta_{i3\min}$ $(i=1,6)$

2. MECHANICAL STRUCTURE OF THE WALKING ROBOT WITH MAMMALIAN CONFIGURATION

Mechanical structure of a walking robot should not only imitate the leg structure of living creatures (e.g., insects, spiders), but also take into account the actuating systems properties (e.g., size, weight and power of the motors) and constraints (e.g., size of the body and the leg workspace) [18]. In this paper, the main body is supported by the legs in mammal-like configuration as mammal legs require less joint torques to support the body. All the legs are built on the same design since the single standard leg design has many advantages in terms of design cost, replacements, modularity and so on. The mechanical model is shown in Fig. 1. Each of the six legs consists of three links which are connected by a hip joint and a knee joint. Each of the leg mechanism is attached to the body via a root joint. The walking robot with n legs landing on the ground is a stable mobile platform, whose body and supporting legs constitute a 6 DOF spatial parallel mechanism which means both three dimensional translation and three dimensional rotation can be realized in the workspace of the robot.

Since this paper mainly focuses on the optimal design of the legs, the kinematic model here is derived by defining the reference frames according to the Denavit–Hartenberg convention [19]. In Fig. 2, a graphical representation of the three-jointed robot leg with attached reference frames and corresponding joint variables is given. The base reference frame $(0_0^{(i)} - xyz)$ is attached to the stationary robot body. The Denavit–Hartenberg link parameters based on Fig. 2 are given in Table 1.

3. COMBINED INDEX OF ENERGY CONSUMPTION AND WORKSPACE

3.1. Energy Consumption Index

The leg joints are actuated by brushless DC motors. The functions of actuators can be expressed as below [18: Voltage balance function

$$U_a(t) = R_a i_a(t) + L_a \frac{di_a(t)}{dt} + U_g(t) \tag{1}$$

EMF function

$$U_g(t) = k_E \dot{\theta}_m(t) \tag{2}$$

Electromagnetic torque

$$\tau_M(t) = k_M i_a(t) \tag{3}$$

Function about electromagnetic torque and joint torque

$$\tau_M(t) = \frac{\tau(t)}{\eta N_G} \tag{4}$$

Speed ratio function

$$\dot{\theta}_m(t) = N_G \dot{\theta} N_G(t) \tag{5}$$

in which, k_M is the torque constant, k_E is the EMF constant, R_a and L_a are the armature resistance and inductance, U_g and i_a are the armature voltage and current, N_G is the gear reduction ratio, $\dot{\theta}_m(t)$ and $\dot{\theta}(t)$ are the speed of motor and joint, η is the motor and gear efficiency, $\tau_M(t)$ is the electromagnetic torque and $\tau(t)$ is the joint torque.

The instantaneous power of the driver is

$$P_a(t) = U_a(t) i_a(t) \tag{6}$$

Substituting (1) and (2) into (6), we obtain

$$P_a(t) = R_a i_a^2(t) + L_a i_a(t) \frac{di_a(t)}{dt} + k_E i_a(t) \dot{\theta}_m(t) \tag{7}$$

Substituting (3) and (4) into (7), we have

$$P_a(t) = \frac{R_a}{k_M^2 \eta^2 N_G^2} \tau^2(t) + \frac{\dot{\theta}(t)\tau(t)}{\eta}. \tag{8}$$

Since the inductance is an energy storage element, if the energy is invariant from the beginning to the end of a period, the energy loss of the inductance can be neglected. Then, the instantaneous power of the drive becomes [17]

$$P_a(t) = \frac{R_a}{k_M^2 \eta^2 N_G^2} \tau^2(t) + \Lambda \left(\frac{\dot{\theta}(t)\tau(t)}{\eta} \right). \tag{9}$$

Taking all joints in the leg into consideration, the total energy of a single leg in a walking gait cycle becomes [19]

$$E_p = \int_0^T \sum_{j=1}^{3} \left(\Lambda \left(\frac{\dot{\theta}_j(t)\tau_j(t)}{\eta} \right) + \frac{R_a}{k_M^2 \eta^2 N_G^2} \tau_j^2(t) \right) dt, \tag{10}$$

where $\Lambda(x)$ is defined as

$$\lambda(x) = \begin{cases} x & \text{if} \quad x > 0 \\ 0 & \text{if} \quad x \leq 0 \end{cases} \tag{11}$$

Here, T is cycle time, the duration of each leg's one step cycle in a periodic gait. R_a, k_M, η and N_G are constant. The value of $\dot{\theta}_j(t)$ depends on the trajectory planning. $\tau_j(t)$ is derived by Lagrange's dynamical equations.

Since the structural dimensions $\hat{\mathbf{L}}$ are the parameters to be optimized, the inverse kinematics solution of the leg is formulated as

$$\mathbf{q} = [\theta_1(\hat{\mathbf{L}}, {}^B\mathbf{P}_F)\theta_2(\hat{\mathbf{L}}, {}^B\mathbf{P}_F)\theta_3(\hat{\mathbf{L}}, {}^B\mathbf{P}_F)]^T \in \mathbf{R}^{3\times 1} \tag{12}$$

in which,

$${}^B\mathbf{P}_F = [{}^BP_{Fx}\ \ {}^BP_{Fy}\ \ {}^BP_{Fz}]^T, \quad \hat{\mathbf{L}} = [L_1\ L_2\ L_3]^T.$$

Usually, ${}^B\mathbf{P}_F$ is the position vector of foot tip in the leg reference frame and is given by the gait generation. Then, trajectory planning is achieved through cubic spline function. The rotational angle, angular speed and angular acceleration can be formulated as

$$\mathbf{q}(\hat{\mathbf{L}}, t) = \begin{bmatrix} \theta_1(\hat{\mathbf{L}}, t) \\ \theta_2(\hat{\mathbf{L}}, t) \\ \theta_3(\hat{\mathbf{L}}, t) \end{bmatrix} = \hat{\mathbf{A}}_s(\hat{\mathbf{L}}) \cdot \mathbf{h}(t) \tag{13}$$

$$\dot{\mathbf{q}}(\hat{\mathbf{L}}, t) = \begin{bmatrix} \dot{\theta}_1(\hat{\mathbf{L}}, t) \\ \dot{\theta}_2(\hat{\mathbf{L}}, t) \\ \dot{\theta}_3(\hat{\mathbf{L}}, t) \end{bmatrix} = \hat{\mathbf{A}}_s(\hat{\mathbf{L}}) \cdot \dot{\mathbf{h}}(t) \tag{14}$$

$$\hat{bfq}(\hat{\mathbf{L}}, t) = \begin{bmatrix} \ddot{\theta}_1(\hat{\mathbf{L}}, t) \\ \ddot{\theta}_2(\hat{\mathbf{L}}, t) \\ \ddot{\theta}(\hat{\mathbf{L}}, t) \end{bmatrix} = \hat{bfA}_s(\hat{\mathbf{L}}) \cdot \ddot{\mathbf{h}}(t) \tag{15}$$

$$\hat{bfA}_s(\hat{\mathbf{L}}) = \begin{bmatrix} a_{10}(\hat{\mathbf{L}})\ a_{11}(\hat{\mathbf{L}})\ a_{12}(\hat{\mathbf{L}})\ a_{13}(\hat{\mathbf{L}}) \\ a_{20}(\hat{\mathbf{L}})\ a_{21}(\hat{\mathbf{L}})\ a_{22}(\hat{\mathbf{L}})\ a_{23}(\hat{\mathbf{L}}) \\ a_{30}(\hat{\mathbf{L}})\ a_{31}(\hat{\mathbf{L}})\ a_{32}(\hat{\mathbf{L}})\ a_{33}(\hat{\mathbf{L}}) \end{bmatrix} \in \mathbf{R}^{3\times(3+1)} \tag{16}$$

$$\mathbf{h}(t) = [1\ \ t\ \ t^2\ \ t^3]^T \in \mathbf{R}^{(3+1)\times 1} \tag{17}$$

$\hat{\mathbf{A}}_s(\hat{\mathbf{L}})$ can be calculated through the initial and final state of the rotational angle and angular speed, but it is still a function with reference to $\hat{\mathbf{L}}$ and t.

For the joint torque

$$\hat{\theta}_p(\hat{\mathbf{L}}, t) = \hat{\mathbf{D}} \cdot \ddot{\mathbf{q}}(\hat{\mathbf{L}}), t) + \hat{\mathbf{C}} \tag{18}$$

$$\hat{\mathbf{D}}(\hat{\mathbf{L}}, \mathbf{q}) = \begin{bmatrix} 0 & 0 & 0 \\ 0 & 1/4m_3L_2^2 + I_2 + m_3L_2^2 & 1/2m_3L_2L_3c_3 \\ 0 & 1/2m_3L_2L_3\ddot{\theta}_2c_3 & 1/4m_3L_3^2 + I_3 \end{bmatrix} \tag{19}$$

$$\hat{\mathbf{H}}(\hat{\mathbf{L}}, \mathbf{q}, \dot{\mathbf{q}}) = \begin{bmatrix} 0 \\ -1/2m_3L_2L_3\dot{\theta}_2s_3 - 1/4m_2L_2^2\dot{\theta}_2 - I_2\dot{\theta}_2 - m_3L_2^2\dot{\theta}_2 - 1/2m_3L_2L_3\dot{\theta}_3c_3 \end{bmatrix} \tag{20}$$

$$\hat{\mathbf{C}}(\hat{\mathbf{L}}, \mathbf{q}) = \begin{bmatrix} 1/2m_2gL_2s_2s_1 + m_3gL_2s_2s_1 + 1/2m_3gL_3s_{23}s_1 \\ -m_2gL_2c_1c_2 - m_3gL_2c_1c_2 - 1/2m_3gL_3c_1c_{23} \\ -1/2m_3gL_3c_1c_{23} \end{bmatrix} \tag{21}$$

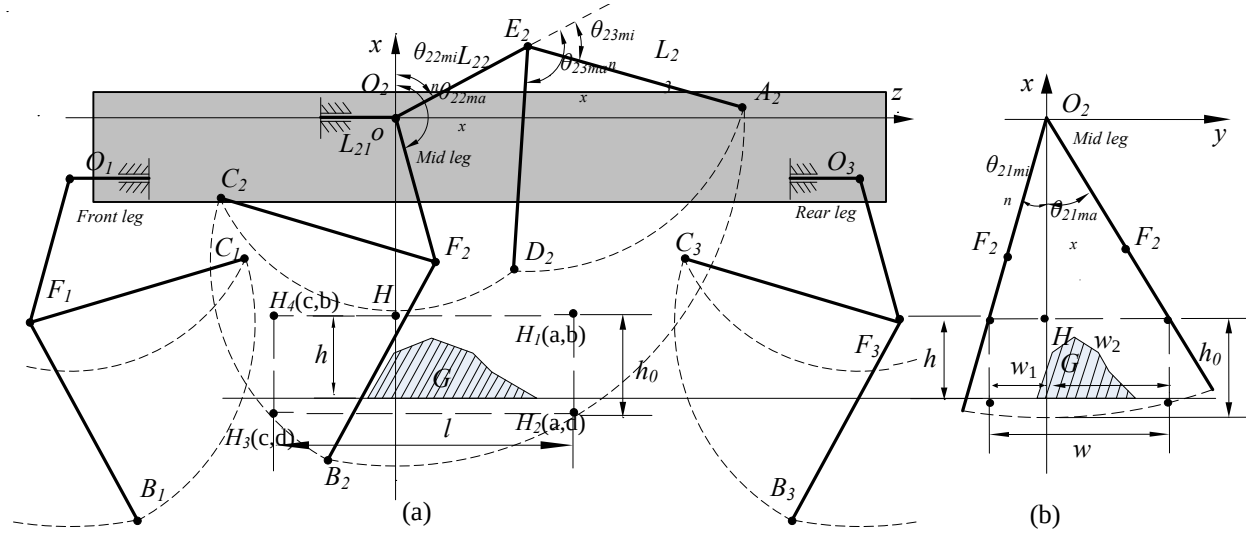

Fig. 3. Analysis of workspace (a) left side view of mid leg (b) front side view of mid leg.

$\hat{\mathbf{D}}(\hat{\mathbf{L}},\mathbf{q})$ is the acceleration related symmetric matrix, which involves the inertia tensor, $\hat{\mathbf{H}}(\hat{\mathbf{L}},\mathbf{q},\dot{\mathbf{q}})$ is the coriolis and centrifugal matrix, $\hat{\mathbf{C}}(\hat{\mathbf{L}},\mathbf{q})$ is the gravity matrix. They are all functions with reference to $\hat{\mathbf{L}}$ and t.

Then, the instantaneous power and the total energy consumption of the three-jointed leg system can be formulated as follows

$$\breve{P}(\hat{\mathbf{L}},t)=\sum_{j=1}^{3}P_j(\hat{\mathbf{L}},t)=\hat{\tau}_p(\hat{\mathbf{L}},t)^T\hat{\mathbf{Q}}_p\hat{\tau}_p(\hat{\mathbf{L}},t)+\max\{c_p^T\hat{\tau}_p(\hat{\mathbf{L}},t),0\} \tag{22}$$

$$\breve{E}_p(\hat{\mathbf{L}})=\int_0^T P(\hat{\mathbf{L}},t)dt=\int_0^T\sum_{j=1}^{3}P_j(\hat{\mathbf{L}},t)dt=\int_0^T(\hat{\tau}_p(\hat{\mathbf{L}},t)^T\hat{\mathbf{Q}}_p\hat{\tau}_p(\hat{\mathbf{L}},t)+\max\{\hat{c}_p^T\ \hat{\tau}_p(\hat{\mathbf{L}},t),0\})dt, \tag{23}$$

where

$$\hat{\mathbf{Q}}_p=\frac{2R}{k_M^2\eta^2N_G^2}\mathbf{E}_3,\quad \hat{\mathbf{c}}_p=\begin{bmatrix}\dfrac{\dot{\theta}_1(\hat{\mathbf{L}},t)}{\eta} & \dfrac{\dot{\theta}_2(\hat{\mathbf{L}},t)}{\eta} & \dfrac{\dot{\theta}_3(\hat{\mathbf{L}},t)}{\eta}\end{bmatrix}^T.$$

It can be known from above that the system energy consumption is a function with reference to $\hat{\mathbf{L}}$ and t. However, since no constraints about the value of the structural parameters are mentioned, no analytical solution can be obtained. Thus, in this paper, the workspace of the leg is discussed to give out some constraints.

3.2. Target Workspace Index

Since the robot probably walks on unstructured terrains and uncertain environments, obstacles are inevitable. Generally, the big obstacle can be detected by the sensing system (e.g., visual system, infrared sensor or laser ranging device). But small obstacles can rarely be detected, that is why the robot should have ability to step on or step over small obstacles. As a result, the mechanism should be designed in particular.

According to the robot structure theory, in the base reference frame $(O_0^{(i)}-xyz)$, taking the 2nd leg (mid leg) for example, the workspace of the leg can be analyzed as shown in Fig. 3, in which $O_iE_iA_i(D_i)$ and $O_iF_iB_i(C_i)$ are the extreme positions of the ith leg. The dashed-line enclosed area is the actual workspace of the legs. The root joint mainly controls the turning of the robot; the hip joint and knee joint are mainly

used for the stride and progress. Here, the obstacle G is involved in the cube of $l \times w \times h$, l is determined by stride length, w and h are related to the dimensions of the obstacle that cannot be recognized by the sensing system. The actual workspace must cover the rectangle $w \times h$ in the *plane-oxy* and rectangle $l \times h_0$ in the *plane-oxz*. Thus, the target workspace is the cube of $l \times w \times h_0$ as shown in Fig. 3. For the rectangle $w \times h$, this can be achieved by rotating the root joint with a corresponding angle θ_1 around the z axis, as shown in Fig. 3(b). Hence, the θ_1 should satisfy

$$\begin{aligned} \theta_{1\min} &\geq \operatorname{arctg}(w_1/|\overline{\mathbf{O_2H}}|), \\ \theta_{1\max} &\geq \operatorname{arctg}(w_2/\overline{\mathbf{O_2H}}|) \end{aligned} \tag{24}$$

Therefore, the optimization of the robot linkage parameters is simplified to the study of the rectangular working area covering rectangle $l \times h_0$ in *plane-oxy*. The working area $S_{A_2B_2C_2D_2}$ should cover the target area $S_{H_1H_2H_3H_4}$ without interfering with the working areas of other legs. In view of energy saving and mechanism simplification, minimal linkage length and minimal rotation scope of each link is desired to satisfy the conditions above. Hence, the optimization of these mechanical parameters is to seek an optimal working area with a compacted structure, which is a problem of nonlinear programming with inequality constraints. According to the analysis above, it is supposed that the design optimization of this project is to obtain the most compact mechanical structure. The area of the actual workspace, combined with energy consumption, is selected as a combined index. The combined index will be minimized by the constraints that the actual workspace should cover the target rectangular area $S_{H_1H_2H_3H_4}$ and no interference with neighboring legs. The main parameters of the robot are denoted as

$$\hat{x} = [\mathbf{F}^T \quad \theta_{2\min} \quad \theta_{2\max} \quad \theta_{3\min} \quad \theta_{3\max}]^T \tag{25}$$

In order to calculate the work area in Fig. 3, $S_{O_2E_2A_2B_2C_2}$ should be calculated first, then subtract the other three parts areas: sectorial area $S_{E_2A_2D_2}$ and $S_{O_2C_2D_2}$, triangle area $S_{\Delta O_2E_2D_2}$ [20].

$$\begin{aligned} \bar{S}(\hat{x}) &= \bar{S}_1(\bar{x}) - (\bar{S}_2(\hat{x}) + \bar{S}_3(\hat{x}) + \bar{S}_4(x)) \\ \bar{S}_1(\hat{x}) &= \bar{S}_5(\hat{x}) + \bar{S}_6(\hat{x}) + \bar{S}_7(\hat{x}) + \bar{S}_8(\hat{x}) \end{aligned} \tag{26}$$

where $\bar{S}(\hat{x}), \bar{S}_1(\hat{x}), \bar{S}_2(\hat{x}), \ldots, \bar{S}_9(\hat{x})$ stands for

$$S_{A_2B_2C_2D_2}, S_{O_2E_2A_2B_2C_2}, S_{E_2A_2D_2}, S_{O_2C_2D_2}, S_{\Delta O_2E_2D_2}, S_{O_2A_2B_2}, S_{\Delta O_2E_2A_2}, S_{F_2B_2C_2}, S_{\Delta O_2C_2F_2}, S_{\Delta O_2C_2F_2}, S_{\Delta O_2F_2B_2}$$

respectively. It is not difficult to verify that

$$\bar{S}_6(\hat{x}) = \bar{S}_9(\hat{x}), \quad \bar{S}_7(\hat{x}) = \bar{S}_2(\hat{x}), \quad \bar{S}_8(\hat{x}) = \bar{S}_4(\hat{x}). \tag{27}$$

Arranging all the equations above, we obtain

$$\bar{S}(\hat{x}) = \bar{S}_5(\hat{x}) - \bar{S}_3(\hat{x}). \tag{28}$$

The sectorial area can be obtained in the Eq. (29), $\bar{\mathbf{e}}_x$ is an unit vector of *axes-x*

$$\begin{aligned} barS_5(\hat{x}) &= \int_0^{|\overline{\mathbf{O_2A_2}}|} (\varphi_B - \varphi_A) r dr, \\ \bar{S}_3(\hat{x}) &= \int_0^{|\overline{\mathbf{O_2C_2}}|} (\varphi_D - \varphi_C) r dr, \\ \cos\varphi_A &= \frac{\overline{\mathbf{O_2A_2}} \cdot \bar{e}_x}{|\overline{\mathbf{O_2A_2}}|}, \quad \cos\varphi_B = \frac{\overline{\mathbf{O_2B_2}} \cdot \bar{e}_x}{|\overline{\mathbf{O_2B_2}}|}, \\ \cos\varphi_C &= \frac{\overline{\mathbf{O_2C_2}} \cdot \bar{e}_x}{|\overline{\mathbf{O_2C_2}}|}, \quad \cos\varphi_D = \frac{\overline{\mathbf{O_2D_2}} \cdot \bar{e}_x}{|\overline{\mathbf{O_2D_2}}|}. \end{aligned} \tag{29}$$

Substituting (29) into (28), the working area $\bar{S}(\hat{x})$ can be calculated by

$$\bar{S}(\hat{x}) = \int_0^{|\overline{\mathbf{O_2A_2}}|} (\varphi_B - \varphi_A) r dr - \int_0^{|\overline{\mathbf{O_2C_2}}|} (\varphi_D - \varphi_C) r dr \tag{30}$$

3.3. Constraints of the Optimization

Since the rectangular area $l \times h_0$ should be included completely in the actual working area $S_{A_2B_2C_2D_2}, \forall \boldsymbol{\sigma}(x,y) \in \hat{\mathbf{N}} \rightarrow \boldsymbol{\sigma}(x,y) \in \hat{\mathbf{M}}$ in which, $\boldsymbol{\sigma}(x,y)$ is a point, $\hat{\mathbf{N}}$ is the point set of $S_{H_1H_2H_3H_4}$, $\hat{\mathbf{M}}$ is the point set of $S_{A_2B_2C_2D_2}$. To satisfy Eq. (31), some inclusion relation constraints should be obeyed.

$$\begin{aligned}
&|\overline{\mathbf{O_2H_1}}| \geq |\overline{\mathbf{O_2\sigma_1}}| \cap |\overline{\mathbf{E_2H_1}}| \geq |\overline{\mathbf{E_2\sigma}}|,\\
&|\overline{\mathbf{O_2H_2}}| \leq |\overline{\mathbf{O_2\sigma_2}}|,\\
&|\overline{\mathbf{O_2H_3}}| \leq |\overline{\mathbf{O_2\sigma_3}}| \cap |\overline{\mathbf{F_2H_3}}| \leq |\overline{\mathbf{F_2\sigma_3}}|,\\
&|\overline{\mathbf{O_2H_4}}| \geq |\overline{\mathbf{O_2\sigma_4}}|,\\
&|\overline{\mathbf{O_2H}}| \geq |\overline{\mathbf{O_2\sigma_2}}|.
\end{aligned} \tag{31}$$

Inclusion relation constraints: (32) Additionally, interferences with neighboring legs are not allowed. Boundary position points C_1 and C_3 of 1th and 3rd leg should not be included in $S_{A_2B_2C_2D_2}$.

Noninterference constraints

$$|\overline{\mathbf{O_2C_3}}| \geq |\overline{\mathbf{O_2\sigma_4}}| \cap |\overline{\mathbf{F_2C_1}}| \geq |\overline{\mathbf{F_2\sigma_3}}| \tag{32}$$

$$|\overline{\mathbf{O_2C_3}}| \geq |\overline{\mathbf{O_2\sigma_4}}| \cap |\overline{\mathbf{F_2C_1}}| \geq |\overline{\mathbf{F_2\sigma_3}}| \tag{33}$$

where σ_1, σ_2, σ_3, σ_4 are the points on the arc $\overset{\frown}{\mathbf{A_2B_2}}$, $\overset{\frown}{\mathbf{B_2C_2}}$, $\overset{\frown}{\mathbf{C_2D_2}}$, $\overset{\frown}{\mathbf{D_2A_2}}$, respectively. All the above vectors can be transformed to the functions with reference to $\hat{x}$.

The boundary constraints must be taken into consideration

$$\hat{x}_{\min} \leq \hat{x} \leq \hat{x}_{\max} \tag{34}$$

$$L_1 + L_2 + L_3 \leq L_{\max}. \tag{35}$$

Thus, the optimization problem should be solved through combining the energy consumption index and target workspace index, and it can be described as follows:

$$\left.\begin{array}{l}
\text{Object Function} \rightarrow \\
\quad \min_{\dot{x}}(F(\hat{x})) = \min_{\dot{x}}(\breve{E}_p(\hat{x}) + \beta \bar{S}(\hat{x})) \\
\text{Minimize} \quad \breve{E}_p(\hat{x}) + \beta \bar{S}(\hat{x}) \\
\text{Subject to} \quad C_k(\hat{x})
\end{array}\right\} \tag{36}$$

in which β is a weighting coefficient, C_k indicates all the inequality constraints in Eqs. (31–35).

4. OPTIMIZATION BASED ON GENETIC ALGORITHM

The genetic algorithm is used for solving this constrained optimization problem. It is based on natural selection, a process that drives the biological evolution. It is widely used in optimization problems for the reason that it is robust to the ill-condition in optimization and it can find global solutions [21]. The method can be presented in Fig. 4.

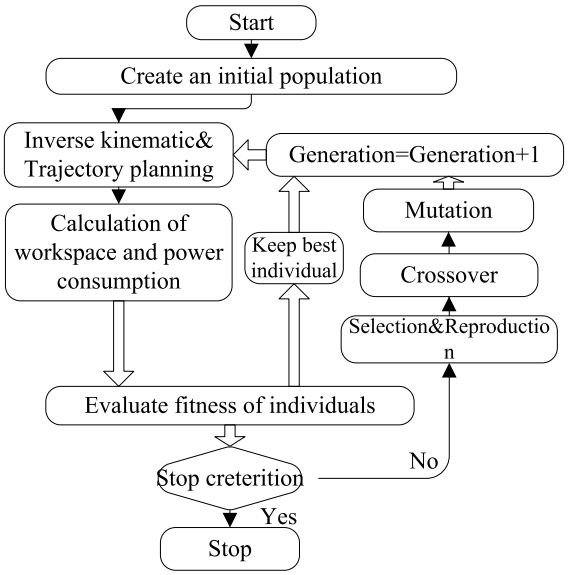

Fig. 4. Process of GA.

1. When a new population is created, new structural parameters of the robot will be selected and it is necessary to restart the trajectory planning process. In one gait period, the initial starting point and the final touching point are generated by the tripod gait [16]. For every single individual, the initial and final joint rotor angles can be solved out by the inverse kinematics function. According to the initial and final conditions, the initial and final joint angles, angular speeds and angular accelerations are obtained by trajectory planning using cubic spline curves Eqs. (13–15).

2. The joint angular speed and angular acceleration are generated by the trajectory planning. The joint torque can be calculated using Eq. (18), then the whole energy consumption in one gait period can be calculated and the workspace can be specified. According to the constraint conditions, punishment factors are given and fitness is evaluated. The inferior individuals of the population are removed and the best one is preserved to the next generation directly.

3. If the stopping criterion is satisfied after evaluating the fitness, the calculation will stop. Otherwise, the evolution of the population will be conducted and the individuals of the population will be selected to create the next generation after selection, reproduction, crossover, and mutation.

In this paper, the parameters of the system are shown in Table 2. The target workspace is supposed to be $l \times w \times h_0$ m^3, the body height is B_H, the horizontal distance between the legs are O_1O_2, O_2O_3, respectively, the gait cycle time is T, the duty factor is B, which stands for the ratio of the duration from the support phase to full stepping in a periodic gait. The stride length is S, the lift height of foot-tip is h_l, the boundary of the variations is specified as $[0,0,0,90^\circ,0,90^\circ]^T \le \hat{x} \le [250,250,90^\circ,270^\circ,90^\circ,180^\circ]^T$ and $L_2+L_3 \le L_{\max}$. The computation stopped when the change of the fitness is smaller than 10^{-6} after 30 generations, the final result is shown below:

$$\begin{cases} \hat{x}_{op} = [50,103,141.8,74.1^\circ,168^\circ,49^\circ,148^\circ]^T \\ [\theta_{1\min},\theta_{1\max}]^T = [-35^\circ,45^\circ]^T \end{cases} \tag{37}$$

The result of the optimization above is compared with $\hat{x}_{ws}$, which is optimized using only workspace index. The value is shown as follows

$$\hat{x}_{ws} = [50,121.5,128.5,76^\circ,170^\circ,42^\circ,133^\circ]^T. \tag{38}$$

Table 2. Parameters of the system.

Parameters	Value	Unit	Parameters	Value	Unit
K_e	13.4	m/Nm/A	l	0.18	m
R_a	9.17	Ω	w	0.17	m
N_G	200	-	h_0	0.10	m
η_G	90.4	-	B_H	0.2	m
η	0.7	-	$L_{\max}$	0.3	m
k_M	13.4	mV/rpm	T	1	s
$I_2(I_3)$	0.375	10^{-3}Kg · m^2	B	0.6	–
β	1	–	S	0.18	m
O_1O_2	0.1	m	h_l	0.05	m
O_2O_3	0.3	m			

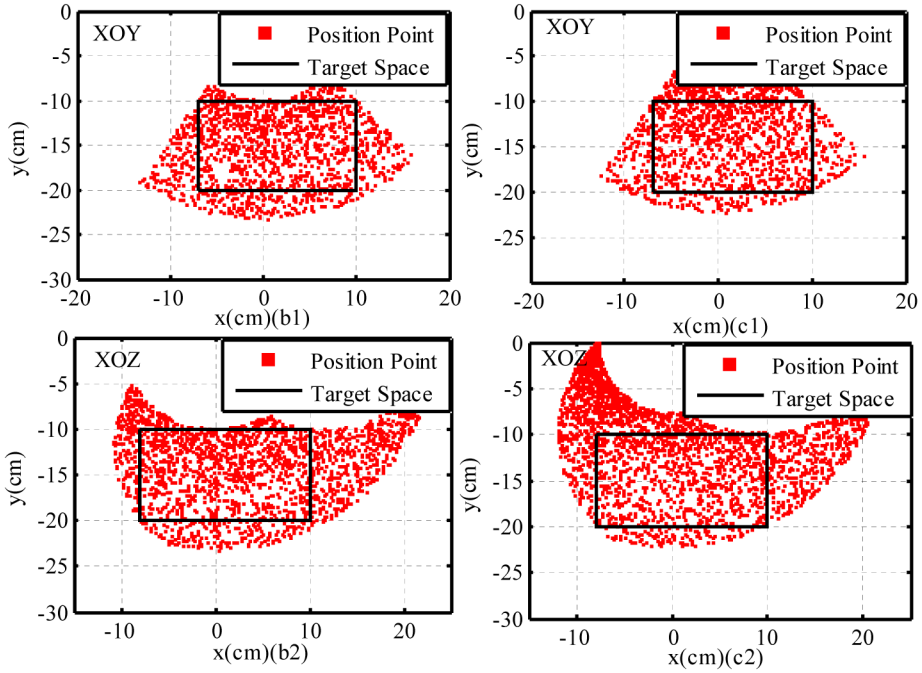

Fig. 5. Actual workspace with different $\hat{x}$: (b) is for $\hat{x}_{ws}$,(c) is for $\hat{x}_{op}$.

The workspace of the two methods is shown in Fig. 5 [22]. Both methods can envelope the target workspace compactly, among which, $\hat{x}_{ws}$ has the optimal workspace. Although the workspace of $\hat{x}_{op}$ isn't the optimal one, it is also very reasonable and acceptable.

The joint torque in one gait period is shown in Fig. 6. It is obvious that optimal design achieves lower joint torque in one period and lower torque impact through transition from swing phase to supporting phase. Although the energy consumption index is not used in the optimization process of $\hat{x}_{ws}$, smaller linkage dimensions and joint rotor angles still make contribution to reducing the energy consumption. However, $\hat{x}_{op}$ makes a more rational distribution of the structural dimensions and achieves higher energy consumption reduction.

Figure 7 shows the instantaneous power consumption of the hip joint and the knee joint and the total energy consumption of a single leg in one gait period. Both the instantaneous power consumption and the joint angular speed are related to the load torque according to Eq. (9), which indicates that smaller link

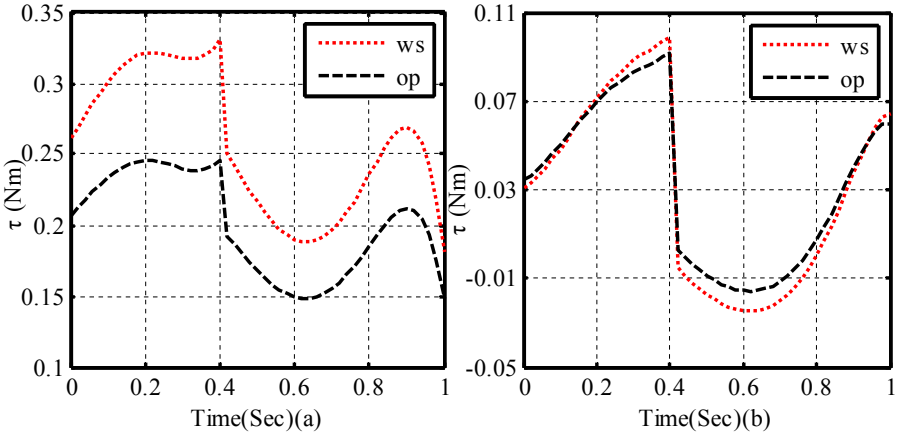

Fig. 6. Joint torque with different $\hat{x}$, (a) is hip joint torque and (b) is knee joint torque.

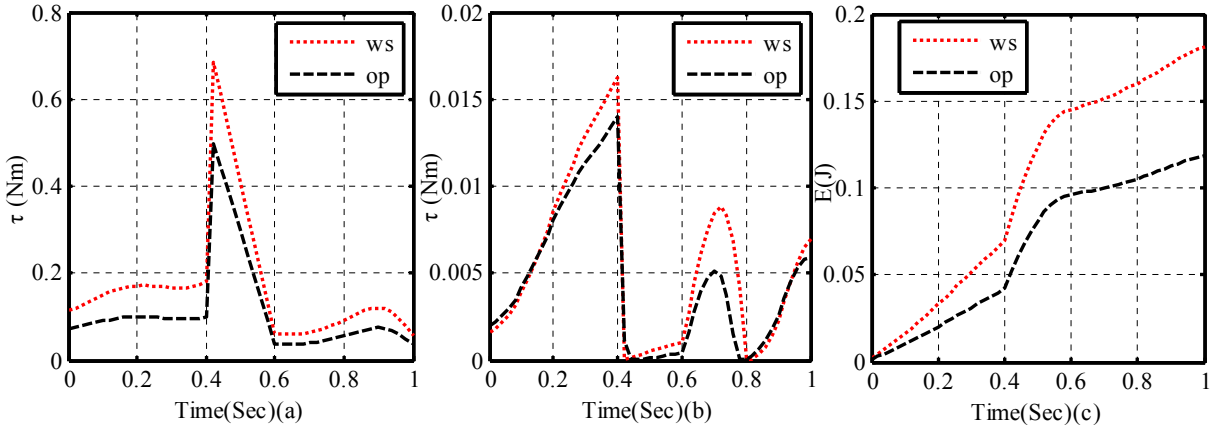

Fig. 7. Joint instantaneous power and total energy consumption with different $\hat{x}$, (a) and (b) is instantaneous energy of hip joint and knee joint, (c) is total energy consumption of a single leg.

dimensions also can generate higher instantaneous power consumption if angular speed is high. That is why $\hat{x}_{op}$, which has a bigger second linkage dimension compared with $\hat{x}_{ws}$, gets a lower instantaneous power consumption. Thus, in the view of instantaneous power consumption, $\hat{x}_{op}$ is better than $\hat{x}_{ws}$ as it is shown in Fig. 7(b). Since the hip joint has greater angular speed and higher load torque and does positive work all the time, it possesses much more instantaneous power consumption than that of the knee joint. This is related to the method of trajectory planning. It is not the key point of this paper. But no matter what kind of method is used to conduct trajectory planning, the mechanism optimization can be achieved by using the optimal design method proposed in this paper. Figure 7(c) reveals that the optimization algorithm combined with energy consumption index can obviously reduce the system energy consumption of a single leg. The total system energy consumption of a single leg $\check{E}_{op}$ decreases 33.4% compared with $\check{E}_{ws}$ in one gait period. Through the analysis of the optimal design method, it can be realized that, not only the target workspace can be enveloped compactly, but also the optimal system energy consumption can be obtained.

5. CONCLUSIONS

A hexapod walking robot with mammalian configuration is designed in this paper. The instantaneous power consumption function and the total energy consumption function of a single leg in one gait period are derived

and the energy consumption index is proposed. Through the analysis of the robot workspace, joint energy consumption index and workspace index are combined and used to derive the objective function. Then, the genetic algorithm coupled with inverse kinematics and trajectory planning in a gait period is used to solve the problem. The results show that the single leg structure optimized by the combined optimization index not only meets the requirements of the system target workspace, but also achieves lower joint torque, instantaneous power consumption and total system energy consumption. This is very important for the hexapod in performing outdoor tasks.

So far, this paper has raised the optimization approach and proved that it is valid and effective. Since the base G.A method is used, more advanced algorithm can be utilized to achieve better performance in further research. Although both the energy consumption index and workspace index are based on the leg structure of a hexapod walking robot, this method is based on motor models and specific workspace. So it can also be used to the optimization of other joint robots.

ACKNOWLEDGEMENTS

This paper is supported by Science Fund for Creative Research Groups of National Natural Science Foundation of China (No. 51221004) and Program for Zhejiang Leading Team of S&T Innovation (Grant No. 2010R50036).

REFERENCES

1. Bares, J.E. and Wettergreen, D.S., "Dante II: Technical description, results, and lessons learned", *The International Journal of Robotics Research*, Vol. 18, No. 7, pp. 621–649, 1999.
2. Gonzalez De Santos, P., Cobano, J.A., Garcia E., et al., "A six-legged robot-based system for humanitarian demining missions", *Mechatronics.* Vol. 17, No. 8, pp. 417–430, 2007.
3. Huang, Q.J. and Nonami, K., "Humanitarian mine detecting six-legged walking robot and hybrid neuro walking control with position/force control", *Mechatronics*, Vol. 13, No. 8, pp. 773–790, 2003.
4. Wettergreen, D., Thorpe, C. and Whittaker, R., "Exploring Mount Erebus by walking robot", *Robotics and Autonomous Systems*, Vol. 11, No. 3, pp. 171–185, 1993.
5. Jin, B., Zhao, L-J., Zhang, J.-L., et al., "Design of the control system for a hexapod walking robot", in *Proceedings of 2011 Second International Conference on Digital Manufacturing and Automation (ICDMA)*, Zhangjiajie, Hunan, China , pp. 401–404, 2011.
6. Saranli, U., Buehler, M. and Koditschek, D.E., "Rhex: A simple and highly mobile hexapod robot", *The International Journal of Robotics Research*, Vol. 20, No. 7, pp. 616–631, 2001.
7. Kar, D.C., "Design of statically stable walking robot: A review", *Journal of Robotic Systems*, Vol. 20, No. 11, pp. 671–686, 2003.
8. Klaassen, B., Linnemann, R., Spenneberg, D., et al., "Biomimetic walking robot SCORPION: Control and modeling", *Robotics and Autonomous Systems*, Vol. 41, No. 2, pp. 69–76, 2002.
9. Gosselin C., Angeles J., "A global performance index for the kinematic optimization of robotic manipulators", *Journal of Mechanical Design*, Vol. 113, No. 3, pp. 220–226, 1991.
10. Lan. P., Liu, M., Lu, N., et al., "Optimal design of a novel high speed and high precision 3-DOF manipulator", in *Proceedings IEEE International Conference on Mechatronics, 2005 ICM'05*, Taipei, Taiwan, pp. 689–694, 2005.
11. Liu, H., Huang, T., Mei, J., et al., "Kinematic design of a 5-DOF hybrid robot with large workspace/limb-stroke ratio", *Journal of Mechanical Design*, Vol. 129, No. 5, pp. 530-537, 2007.
12. Hwang, Y.K., Yoon, J.W. and Ryu, J.H., "The optimum design of a 6-dof parallel manipulator with large orientation workspace", *Proceedings of IEEE International Conference on Robotics and Automation, 2007*, Busan, Korea, pp. 163–168, 2007.
13. Oetomo, D., Daney, D. and Merlet, J.P., "Design strategy of serial manipulators with certified constraint satisfaction", *IEEE Transactions on Robotics*, Vol. 25, No. 1, pp. 1–11, 2009.

14. Zielinska, T. and Heng, J., "Development of a walking machine: Mechanical design and control problems", *Mechatronics*, Vol. 12, No. 5, pp. 737–754, 2002.
15. Gonzalez De Santos, P., Garcia, E. and Estremera, J., "Improving walking-robot performances by optimizing leg distribution", *Autonomous Robots*, Vol. 23, No. 4, pp. 247–258, 2007.
16. Jin, B., Hu, S. and Yu, Y-X., "Design of novel hexapod walking robot", *Mechanical & Electrical Engineering Magazine*, Vol. 24, No. 6, pp. 23–25, 2007.
17. Jin, B., Chen, C. and Li, W., "Power consumption optimization for a hexapod walking robot", *Journal of Intelligent & Robotic Systems*, Vol. 71, No. 2, pp. 195–209, 2013.
18. Zielinska, T. and Heng, J., "Development of a walking machine: Mechanical design and control problems", *Mechatronics*, Vol. 12, No. 5, pp. 737–754, 2002.
19. Jin, B., Chen, C. and Li, W., "Optimization of energy-efficient torque distribution for hexapod walking robot", *Journal of Zhejiang University (Engineering Science).* Vol. 46, No. 7, pp. 1168–1174, 2012.
20. Han, S., Xueyan, S., Tiezhong, Z., et al., "Design optimisation and simulation of structure parameters of an eggplant picking robot", *New Zealand Journal of Agricultural Research*, Vol. 50, No. 5, pp. 959–964, 2007.
21. Capi, G., Nasu, Y., Barolli, L., et al., "Application of genetic algorithms for biped robot gait synthesis optimization during walking and going up-stairs", *Advanced Robotics*, Vol. 5, No. 6, pp. 675–694, 2001.
22. Liang, X.-F., Wang, Y.-W., Miao, X.-W., et al., "Analysis and simulation of the workspace of a tomato harvesting manipulator", *Journal of Zhejiang University (Agric. & Life Sci.)*, Vol. 31, No. 6, pp. 807–811, 2005.